Available online at www.sciencedirect.com
SCIENCE DIRECT®
European Polymer Journal 40 (2004) 371–378
EUROPEAN POLYMER JOURNAL
www.elsevier.com/locate/europolj

Crystallisation behaviour of high density polyethylene blends with bimodal molar mass distribution 2. Non-isothermal crystallisation

Andres Krumme [a,*], Arja Lehtinen [b], Anti Viikna [a]

[a] Department of Polymer Materials, Tallinn Technical University, Ehitajate tee 5, 19086 Tallinn, Estonia
[b] Borealis Polymers Oy, P.O. Box 330, FIN-06101 Porvoo, Finland

Received 3 February 2003; received in revised form 6 October 2003; accepted 8 October 2003

Abstract

Crystallisation of high density polyethylene (HDPE) blends with broad bimodal molar mass distribution was investigated by differential scanning calorimetry (DSC) under non-isothermal conditions. The blends were prepared by blending a high molar mass PE ($M_w = 330$ kg/mol, $M_w/M_n = 4.8$) and a low molar mass linear PE ($M_w = 34$ kg/mol, $M_w/M_n = 10$) in different ratios in xylene solution. The samples were analysed by the normal DSC at different crystallisation rates and by a thermal fractionation technique.

The blends and their parent polymers behaved according to general expectations i.e., crystallinity and density decreased when the molar mass of the samples increased. Additionally, non-linear relationships between MM and different analysed parameters were found. Small addition of the high molar mass parent polymer to the low molar mass parent polymer increased crystallisation temperature, although the general trend was decreasing. Furthermore, a complicated relationship between the reciprocal of crystallisation half-time and sample composition was found. The value increased first with increasing molar mass, reached a maximum when the average molar mass of the blend was between 150 and 200 kg/mol and then decreased. The detected maximum correlated with the broadest molar mass distribution of the blends. The crystallinities and densities of the blends with the broadest molar mass distribution also deviated from the linear correlation between them and molar mass. The Avrami index under non-isothermal conditions was analysed with a method developed by Harnisch and Muschik. The results indicated that thermal nucleation and spherical growth regimes are present in all studied materials.

Keywords: High density polyethylene; Bimodal blends; Non-isothermal; Crystallisation; Differential scanning calorimetry; Avrami index; Half-time

1. Introduction

Current paper completes the study of crystallisation of bimodal high density polyethylene (HDPE) blends [1] by non-isothermal crystallisation data. Semicrystalline polymers are invariably processed under continuous cooling (non-isothermal) conditions. Since the morphology thus formed is determining the mechanical and physical properties of the products, information about the crystallisation under non-isothermal conditions is of practical significance.

The polymer blends in this study simulate materials produced with a Ziegler–Natta catalyst in cascaded reactors. Production of this kind of bimodal HDPE materials is increasing. This type of catalyst-process combination gives the possibility to tailor both molar mass distribution and incorporation of comonomer as a

* Corresponding author. Tel.: +372-6202907; fax: +372-6202903.
E-mail address: krumts@staff.ttu.ee (A. Krumme).

0014-3057/$ - see front matter © 2003 Elsevier Ltd. All rights reserved.
doi:10.1016/j.eurpolymj.2003.10.004

function of molar mass (MM), and in that way both change the crystallisation behaviour and improve processability, impact properties and stress crack resistance of the materials [2–5]. Bimodal polyethylenes with better mechanical properties have displaced unimodal chromium-based HDPE resins and become the industry standard in such applications as pressure pipes, film and blow moulding.

In this study we have systematically investigated the crystallisation behaviour of HDPE blends having broad, bimodal molar mass distributions and various compositions. The target was to increase basic knowledge about the parameters having an influence on the crystallisation behaviour of bimodal polyethylene. The first part of this work was devoted to the structural characterisation of the blends and to the study of their isothermal crystallisation [1]. This second paper complements the isothermal crystallisation data with non-isothermal crystallisation kinetics, crystallinity and crystallisation/melting temperatures.

2. Experimental

2.1. Materials

The parent polymers of the blends studied were a low molar mass (LMM) linear polyethylene ($M_w = 34100$ g/mol, $M_w/M_n = 10$) and a high molar mass (HMM) PE containing 0.6 wt% of 1-hexene as a comonomer ($M_w = 330000$ g/mol, $M_w/M_n = 4.8$). Both polymers were produced with a Ziegler–Natta catalyst in a pilot scale slurry loop reactor by Borealis Polymers OY. The blends were prepared by solution blending and the blending procedure together with the compression moulding of thin plates is described elsewhere [1]. The parent polymers were either analysed as they arrived from the production (overall crystallisation behaviour) or given the same solution treatment as the blends (effect of cooling rate and crystallisation kinetics). Detailed structural characterisation of the blends and their parent polymers was carried out in the first part of this work [1]. Their main molecular characteristics are reported in Table 1. The solution treatment did not change M_w and MMD of the HMM parent polymer. The MMD of the LMM component was slightly narrowed when some wax-like material was lost in the dissolution and precipitation steps. Effect of the solution blending on crystallisation of the parent polymers is also described elsewhere [6].

2.2. Differential scanning calorimetry

Crystallisation and melting behaviour under non-isothermal conditions were investigated by DSC using a Mettler Toledo DSC 822^e equipped with a mechanical intracooler and purged with nitrogen. The temperature scale of the calorimeter was calibrated with water, indium and lead, and the thermal response from the melting enthalpy of indium. The calibration was checked with several heating rates and the calibration carried out at 10 °C/min was found to be accurate enough also for all other scan rates used.

The experiments for determining standard melting and crystallisation behaviour for structural characterisation were carried out with 3.2 ± 0.2 mg of samples cut from the middle of the melt pressed plates. All samples were first melted at 180 °C for 5 min, cooled to 0 °C at a rate of 10 °C/min and then reheated from 0 to 180 °C at a rate of 10 °C/min. Crystallisation and melting temperatures were obtained from the cooling and second-heating thermograms, respectively. The degree of crystallinity was determined from the melting endotherm. The weight crystallinity θ_w was calculated by Eq. (1):

$$\theta_w = \frac{\Delta H_m}{\Delta H_m^0}, \tag{1}$$

where ΔH_m is the melting enthalpy calculated from the area of the melting endotherm and ΔH_m^0 is enthalpy of fusion of 100% crystalline PE ($\Delta H_m^0 = 290$ J/g) [7].

Table 1
Molecular characteristics of the blends and their components

HMM PE content (wt%)	M_w (g/mol)	M_w/M_n	T_m (°C)	θ_w (%)	T_m[a] (°C)	θ_w[a] (%)	ρ (kg/m^3)
0	34 100	10.0	129.8	85.3	134.0	89.8	973.0
20	82 800	12.7	132.3	80.5	135.9	87.7	966.9
40	140 000	17.7	133.5	75.3	137.8	83.7	963.1
45	151 000	19.6	133	75.1	137.6	83.7	962.3
50	181 000	21.8	132.7	72.8	136.9	82.4	960.9
55	189 000	21.2	133.0	71.9	137.2	79.5	959.8
60	195 000	20.7	132.6	70.0	137.5	79.0	957.0
80	264 000	13.7	132.5	64.4	137.8	72.3	951.0
100	330 000	4.8	132	58.5	136.5	65.7	942.3

[a] Obtained after thermal fractionation by stepwise isothermal crystallisation.

In the thermal fractionation experiments the samples of 3.5 ± 0.5 mg (cut from the melt pressed plates) were first melted at 180 °C for 5 min, fast cooled to 131 °C and then cooled at a rate of 10 °C/min to the first crystallisation temperature (126 °C) and held there for 90 min. The next steps in this stepwise crystallisation were 121 °C (80 min), 116 °C (60 min), 111 °C (50 min) and 106 °C (30 min), and the samples were cooled at 10 °C/min between the steps. After the last annealing step the samples were cooled to 0 °C at a rate of 10 °C/min. The heating scans were obtained by heating the thermally fractionated samples from 0 to 180 °C at a rate of 10 °C/min. Melting temperatures and degree of crystallinity were determined from the melting endotherms obtained.

To reduce thermal lag upon scanning in the non-isothermal crystallisation kinetics studies, the sample mass used was 2 ± 0.1 mg. Sample disks of about 0.14 mm thickness and 4.5 mm diameter were employed to obtain the best contact with the aluminium sample pan. Details of the sample discs preparation are presented in [1]. For kinetic studies the samples were first melted at 180 °C under nitrogen for 5 min to erase previous thermal history. Then they were cooled at a rate of 1, 5, 10 or 20 °C/min to 0 °C and subsequently remelted at a heating rate of 10 °C/min over the temperature range 0–180 °C. The T_c, T_m and crystallinity values obtained are presented in Table 2.

3. Results and discussion

3.1. General crystallisation behaviour

As mentioned in the experimental part, the general melting/crystallisation behaviour of the blends and their components was determined by DSC using specimens cut directly from the melt pressed plates. In all measurements the heating rate was 10 °C/min, while different thermal histories were obtained by crystallising the samples at cooling rate 10 °C/min or using a thermal fractionation technique. The crystallisation exotherms of the blends and their parent polymers at cooling rate 10 °C/min are presented in Fig. 1. This figure shows the effect of blend composition on the shape of the crystallisation exotherm. The blends had only a single crystallisation or melting peak and the width of this peak varied somewhat with the blend composition.

The thermal fractionation technique is often used to provide information about the structural heterogeneity of ethylene copolymers and their blends [8,9]. The multiple endotherms obtained can be correlated to lamellar thickness distribution, and lamellar thickness is directly related to the ethylene chain length between branch points. In this work the HMM PE used in the blends contained only 0.6 wt% of 1-hexene as a comonomer (1 butyl branch/1000 carbon atoms) and the LMM component was a linear ethylene homopolymer. This means that the average level of short chain branching in the HMM/LMM PE blends was very low. The calculated comonomer contents varied from about

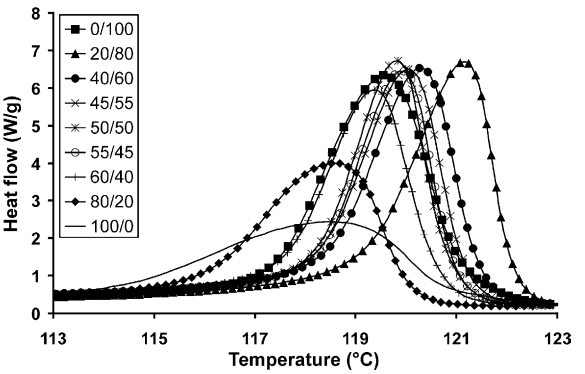

Fig. 1. Crystallisation curves of the blends and their components at cooling rate 5 °C/min.

Table 2
Crystallisation temperature (T_c), melting temperature (T_m) and crystallinity (θ_w) of the blends and their components at different cooling rates

HMM PE content (wt%)	1 °C/min			5 °C/min			10 °C/min			20 °C/min		
	T_c (°C)	T_m (°C)	θ_w (wt%)	T_c (°C)	T_m (°C)	θ_w (wt%)	T_c (°C)	T_m (°C)	θ_w (wt%)	T_c (°C)	T_m (°C)	θ_w (wt%)
0	122.2	131.9	87.4	120.5	129.7	83.8	118.8	130.9	80.7	116.9	127.1	79.4
20	123.1	132.1	81.3	120.9	131.3	79.1	119.7	130.7	79.2	118.0	130.7	78.0
40	122.3	132.4	79.3	120.3	131.4	77.9	119.3	131.0	76.4	118.0	130.5	74.7
45	122.1	132.7	77.3	120.0	131.5	76.3	119.1	131.2	75.7	117.8	130.6	70.7
50	121.8	132.6	71.2	119.8	131.2	72.7	118.7	130.8	71.3	117.6	130.4	71.0
55	121.9	132.5	72.8	120.0	131.3	70.3	119.1	130.9	70.6	117.8	130.5	69.7
60	121.6	132.6	70.4	119.4	131.4	70.8	118.6	130.8	67.6	117.2	130.4	67.0
80	121.1	132.6	67.3	118.6	132.4	63.9	117.7	131.2	64.5	116.1	130.7	62.6
100	121.0	132.3	61.3	118.9	132.2	59.6	117.1	131.9	55.2	114.2	131.6	56.0

0.1 wt% for the 20/80 blend to about 0.5 wt% for the 80/20 blend. We observed no thermal fractionation during stepwise isothermal crystallisation experiments, meaning that only one endotherm was obtained by remelting of the treated samples. Therefore from practical point of view the blends were prepared from two HDPE materials having different molar masses and MMDs, and in thermal fractionation the influence of small amount of short chain branching was negligible.

The melting temperatures and crystallinities determined using normal DSC runs and the thermal fractionation technique are summarised in Table 1 and in Figs. 2 and 3. In general, the density and crystallinity of the blends decreased with increasing MM, i.e. with increasing amount of the HMM component. Fig. 2 shows that the decrease was generally linear but the blends containing both parent polymers in about equal ratios (the blends having the highest polydispersity) seem to have slightly higher crystallinity and density than the trendline presents. Specimens with highest crystallinity and melting temperature were, however, obtained by stepwise isothermal crystallisation. In this thermal fractionation technique the samples were crystallised from the melt isothermally at several successively decreasing temperatures. The total crystallisation time was thus several hours allowing formation of thicker, more perfect lamellae and reorganisation of polymer chains in the melt so that a larger part of the macromolecules could crystallise. A good linear correlation was found between blend density and crystallinity calculated from the standard DSC measurements and from the melting endotherms of the thermally fractionated samples (Fig. 3). Specimens for density measurements, standard DSC analyses and thermal fractionation were cut from the same melt pressed plates, but due to the methods used, in the measurements itself they had different thermal histories.

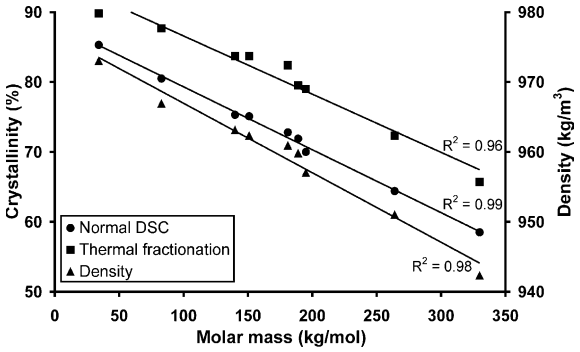

Fig. 2. Crystallinity of the blends as a function of MM for samples having different thermal histories.

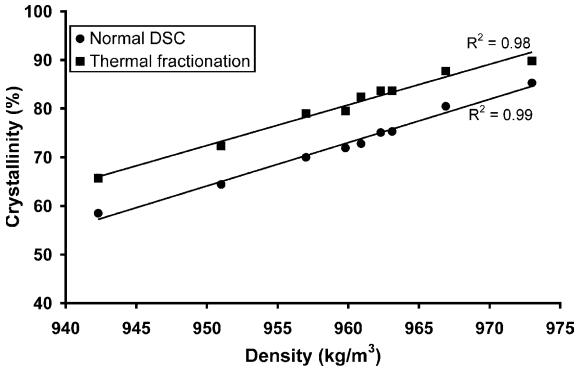

Fig. 3. Correlation between crystallinity and density for samples having different thermal histories.

3.2. Effect of cooling rate

The melting/crystallisation behaviour of the blends and their components at different cooling rates was determined by DSC using the sample disks prepared in the hot-stage. To obtain similar powder morphology for all samples, the parent polymers went through the same solution treatment as the blends. In the non-isothermal crystallisation kinetics studies the sample discs had a lower weight than was used in the normal DSC analyses. This guaranteed a better thermal response at high cooling rates. In general, the DSC samples cut from the melt pressed plates gave broader crystallisation and melting ranges than the corresponding specimens cut from the thin films prepared in the hot-stage. This difference was detected even when in all DSC analyses the samples were first melted at 180 °C for 5 min to erase previous thermal history and then crystallised afresh from the melt. One reason for this type of behaviour might be the different thickness and geometry of the samples. Billon et al. [10] have recently shown that transcrystallisation may occur during DSC measurements of HDPE and therefore the thickness of the sample can have an influence on the crystallisation behaviour and broaden the crystallisation peak, especially at the higher cooling rates. However, light microscopic examination of cross-sections cut from our DSC samples showed no or a minimum effect of transcrystallisation [6], so the peak broadening was probably caused by accumulation of crystallisation heat in thicker samples, as is explained in [1].

As an example, the crystallisation exotherms of the 50/50 HMM/LMM PE blend at different cooling rates are presented in Fig. 4. The crystallisation peak broadened and shifted to lower temperatures when the cooling rate increased. The blends and parent polymers showed only a single crystallisation or melting peak at all cooling rates.

The melting and crystallisation temperatures and crystallinities determined for the samples having differ-

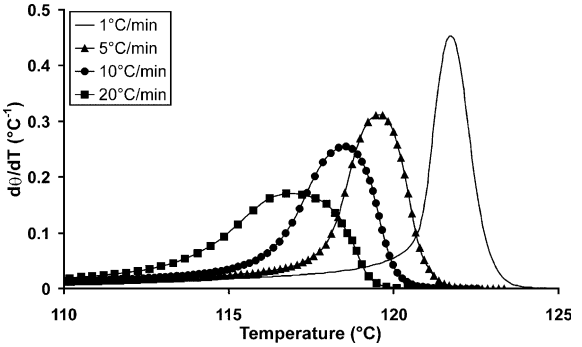

Fig. 4. Crystallisation of the 50/50 HMM/LMM PE blend at different cooling rates (the exotherms ''normalised'' according to the method developed by Billon et al. [10]).

ent thermal histories are summarised in Table 2. The crystallinity of the blends decreased with increasing cooling rate. An increase in the cooling rate also resulted in a clear decrease of crystallisation temperature T_c and the subsequent melting temperature T_m followed the same trend. At the same time the temperature difference between the melting and crystallisation temperatures ($\Delta T = T_m - T_c$) increased. At higher cooling rates a higher degree of undercooling is required for initiating polymer crystallisation and the results obtained reflect this tendency. Influence of the blend composition on the crystallisation temperature was smaller than that of the cooling rate as is shown in Table 2. A small addition of the HMM PE into the LMM linear PE slightly increased the crystallisation temperature of the material. When larger amounts of the HMM component were used, its influence on the MM of the blend increased, at the same time decreasing the crystallisation temperature. The melting temperature of the HMM parent polymer was higher than that of the LMM parent polymer but the melting temperatures of the blends were nearly unaffected by their composition.

The well known Thomson–Gibbs equation [11] was applied for analysing how the blend composition and cooling rate affected the lamellar thickness distribution of the samples. The equation predicts a linear relationship between melting temperature and reciprocal of lamellar thickness

$$L = \frac{2\sigma_e T_m^0}{\Delta H_v (T_m^0 - T_m)}. \quad (2)$$

where T_m^0 is the equilibrium melting temperature of the infinitely thick crystal, σ_e is the fold surface interfacial free energy, ΔH_v is the melting enthalpy per repeating unit and L is the thickness of a lamella that melts at melting temperature T_m [11,12]. Following values of the mentioned parameters were used in this work for PE: $T_m^0 = 414.8$ K [7], $\sigma_e = 93$ mJ/m^2 [11] and $\Delta H_u = 288 \times 10^6$ J/m^3 [8]. The parameter σ_e is not a constant with temperature change and should be determined by other methods before using it in Eq. (2) for the analysis of DSC data [13]. Somewhat varying values can be found in the literature also for the other parameters used in the calculations. Therefore, the mean lamellar thicknesses obtained from Eq. (2) are no absolute values and can only be compared with each other.

We analysed the melting endotherms of the samples crystallised at different cooling rates. These endotherms were recorded at heating rate 10 °C/min. This was a suitable rate due to two reasons: it was high enough to avoid recrystallisation during the melting process, but not too high for causing large error due to thermal lag [14,15]. In the analysis of the DSC melting curves it is assumed, that the rate of heat flow at a given temperature is proportional to the fraction of lamellae with a thickness L [14]. In this work the melting endotherms of the samples were integrated by parts of 5 °C, from 101 up to 141 °C and lamellar thicknesses for these parts were calculated using Eq. (2). The data obtained for the blends and their components indicated that most composition dependent changes in the crystallinity of these blends took place in the T_m range from 121 to 136 °C

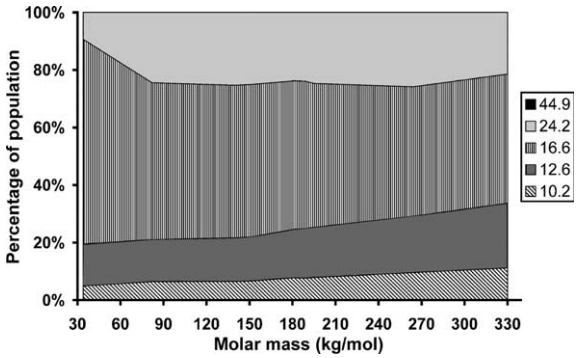

Fig. 5. Lamellar thickness distribution obtained at cooling rate 10 °C/min.

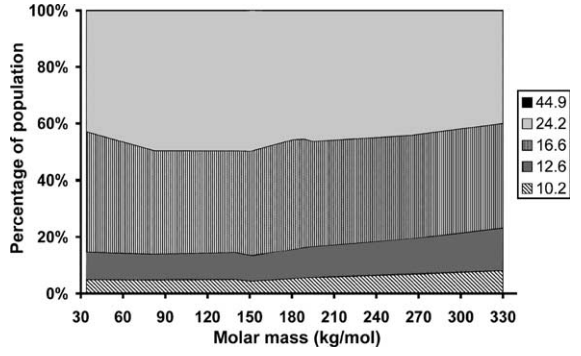

Fig. 6. Lamellar thickness distribution obtained at cooling rate 1 °C/min.

(10.2 nm $< L <$ 44.9 nm). Thinner lamellae were not affected by the changes in the blend composition and the amount of thicker lamellae was less than 0.5 wt%. The calculated lamellar thicknesses correlated well with previous studies of the HDPE lamellar thickness distribution [14–16].

Figs. 5 and 6 present lamellar thickness distributions obtained from the melting endotherms recorded after crystallisation at cooling rates 10 and 1 °C/min. An obvious effect of the lower cooling rate was an increase in dominating lamellar thickness. If at cooling rate 10 °C/min the dominating population had a maximum thickness of 16.6 nm, then at rate 1 °C/min the dominating population had a maximum thickness of 24.2 nm. Also the amount of thinner lamellae decreased. This shift was characteristic for all the materials studied, indicating that under favorable environmental conditions they all were capable of lamellar thickening. Percentage of thicker lamellae decreased slightly when the average molar mass of the samples increased. The lamellar thickness distributions of the blends and their parent polymers showed only small differences.

3.3. Crystallisation kinetics

The Avrami equation [17–19] is probably the most intensively used tool for analysing polymer crystallisation kinetics. We also applied this equation for analysing isothermal crystallisation of our materials [1]. This equation was created for describing crystallisation processes under isothermal conditions and attempts to modify it for non-isothermal conditions (well summarised in [20]) have had variable practical value, depending on the studied material and analysis conditions. A commonly used extension to Avrami's theory was presented by Ozawa [21]. This method can be used when crystallisation occurs at a constant cooling rate. A few attempts to apply Ozawa theory for PE have been published. Determination of crystallisation kinetics of short chain branched PE fractions produced by a metallocene catalyst and having a narrow MMD was successful [22], but the analysis of commercial HDPE with broad MMD failed [23]. In this study the blends and their parent polymers had broad MMDs and the Ozawa method could not be used in their kinetics analysis. No linear correlation between crystallinity and cooling rate was found. This may indicate that at least in the case of PE, the suitability of the Ozawa theory may depend on the width of MMD.

The Avrami equation relates crystalline conversion at certain time to crystallisation rate constant and parameter n which is known as the Avrami index and depends on the type of nucleation and growth dimension. These parameters are widely applied for describing crystallisation kinetics of polymers. Since the rate constant is not physically meaningful under non-isothermal conditions, instead of it we used crystallisation half-time $t_{0.5}$. Parameter n was determined using a method developed by Harnisch and Muschik [24].

The crystallisation half-time is the time the crystallisation starts to the time 50% of relative volume crystallinity is achieved. Reciprocal of the half-time is related to the crystallisation rate constant and we found a good correlation between the reciprocal values and the rate constants obtained under non-isothermal conditions. As expected, the reciprocal of the half-time increased when the cooling rate was higher. A complicated relationship between the average MM and the reciprocal of the crystallisation half-time was obtained (Fig. 7). The value increased first with increasing MM, reached a maximum when the average MM of the blend was between 150 and 200 kg/mol and then decreased. With decreasing cooling rate the correlation approached a linear dependence. The results indicate that in addition to MM itself, the crystallisation rate also depended on the MMD of the blends. The reciprocal of the half-time had a maximum when the blends had the broadest MMD (M_w/M_n values are presented in Table 1).

Similar complicated MM and crystallisation rate relationships have been reported for blends of HMM and ultra high molar mass (UHMM) PE [25] and also for linear PE fractions with narrow MMD [26,27].

Harnisch and Muschik [24] suggested that the Avrami index under non-isothermal conditions can be expressed by the following equation

$$n = 1 + \left[\ln \frac{\dot{\theta}_{v,1}}{1-\theta_{v,1}} - \ln \frac{\dot{\theta}_{v,2}}{1-\theta_{v,2}} \right] \Big/ \ln \frac{\beta_2}{\beta_1}, \qquad (3)$$

where θ_v is the relative volume crystallinity, calculated from the DSC data in the way described in the first part of this study [1], $\dot{\theta}_v$ is the derivative of the relative volume crystallinity and β is the cooling rate. The index n is calculated at certain temperature in the crystallisation range by inserting the crystallinity values and the

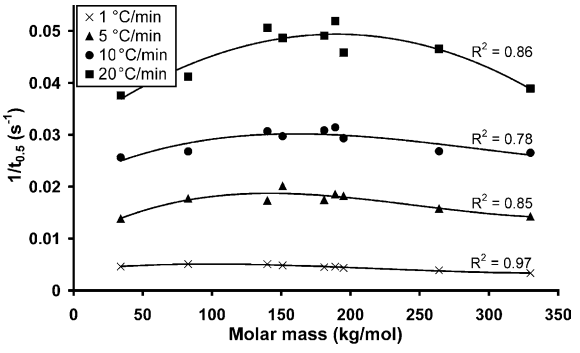

Fig. 7. Reciprocal of crystallisation half-time as a function of the MM of the samples.

derivatives obtained at two different crystallisation rates 1 and 2 into Eq. (3). The method suggests that parallel lines should be obtained if $\ln \dot{\theta}_v/(1-\theta_v)$ vs. T is plotted at different cooling rates. The value of $[\ln \dot{\theta}_{v,1}/(1-\theta_{v,1})] - [\ln \dot{\theta}_{v,2}/(1-\theta_{v,2})]$ in Eq. (3) is then obtained as vertical distance between two of these parallel lines. Fig. 8 presents a typical plot of our data. Straight lines were obtained when the relative crystallinity was between 0 and 30%. A linear fit was not available at higher conversion rates. Furthermore, lines obtained at cooling rate 1 °C/min were excluded, as they did not fit the results obtained at higher crystallisation rates. This indicates that also this method gives reliable results only under certain limitations, and when there is no secondary crystallisation.

The indexes determined are presented in Table 3. Values between 3.4 and 4 were obtained. Wunderlich suggests [7] that the index should decrease by one at certain time if the value is obtained under non-isothermal conditions and the nucleation centres are being exhausted. Accordingly, the values between 3 and 4 correspond to the thermal nucleation and spherical growth regime. The indexes calculated showed high standard deviations, therefore the effect of the MMD on the index could not be determined. The value of n showed a slight decreasing trend when the MM of the samples increased.

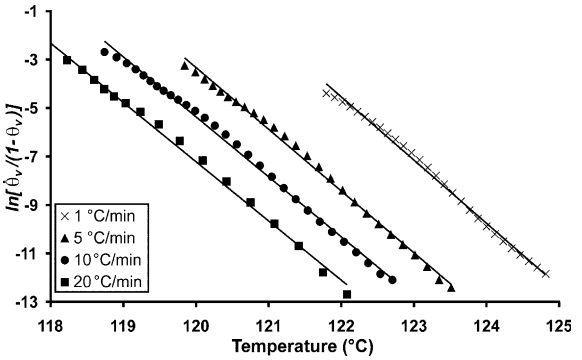

Fig. 8. $\ln \dot{\theta}_v/(1-\theta_v)$ vs. T graphs of the 50/50 HMM/LMM PE blend.

Table 3
The Avrami index (n) values determined for the materials studied

HMM PE content (wt%)	n
0	3.85 ± 0.57
20	4.03 ± 0.11
40	3.73 ± 0.02
45	4.10 ± 0.56
50	3.73 ± 0.15
55	4.10 ± 0.51
60	3.43 ± 0.71
80	3.46 ± 0.05
100	3.73 ± 0.24

4. Conclusions

We found by this study that the blends and their parent polymers generally behaved according to our expectations i.e. crystallinity and density decreased when the molar mass of the samples increased. An increase in the cooling rate also caused a decrease in crystallinity and crystallisation temperature. All DSC thermograms showed only one peak. Both in the isothermal [1] and non-isothermal crystallisation studies we failed to demonstrate clearly what additional effect the small amount of short chain branching present in our blends and in the HMM parent polymer had on our results. However, we can assume that both molar mass and SCB had an effect on the melting and crystallisation temperatures, crystallinity, density and dominant lamellar thickness of our materials, but that the effect of molar mass was the dominating parameter.

Additionally we found that the relationships between MM and different analysed parameters are not always simple and linear. For example, a small addition of the HMM parent polymer to the LMM parent polymer increased crystallisation temperature, although the general trend was decreasing when the average MM increased. A complicated relationship between the reciprocal of crystallisation half-time and sample composition was found. The value increased first with increasing MM, reached a maximum when the average MM of the blend was between 150 and 200 kg/mol and then decreased. The maximum detected correlated with the broadest MMD of the studied blends. The crystallinities and densities of the blends with the broadest MMD also deviated from the linear correlation between them and MM.

After analysing the Avrami index under non-isothermal conditions with a method developed by Harnisch and Muschik we can conclude that thermal nucleation and spherical growth regimes are present in our materials. However, a clear molar mass dependence was not revealed by the results.

References

[1] Krumme A, Lehtinen A, Viikna A. Eur Polym J, in press [doi:10.1016/j.eurpolymj.2003.10.005].
[2] Böhm LL, Enderle HF, Fleissner M. Adv Mater 1992;4:234.
[3] Böhm LL, Enderle HF, Fleissner M. Stud Surf Sci Catal 1994;89:351 [Catalyst design for tailor-made polyolefins].
[4] Sheirs J, Böhm LL, Boot JC, Leevers PS. Trends Polym Sci 1996;4:408.

[5] Hubert L, David L, Seguela R, Vigier G, Degoulet C, Germain Y. Polymer 2001;42:8425.
[6] Krumme A, Lehtinen A, to be submitted.
[7] Wunderlich B. Macromolecular physics. New York: Academic Press; 1976.
[8] Arnal ML, Balsamo V, Ronca G, Sanchez A, Müller AJ, Canizales E, Urbina de Navarro C. J Therm Anal Calorim 2000;59:451.
[9] Zhang F, Fu Q, Lu T, Huang H, He T. Polymer 2002;43:1031.
[10] Billon N, Henaff V, Pelous E, Haudin JM. J Appl Polym Sci 2002;86:725.
[11] Gedde UW. Polymer physics. London: Chapman & Hall; 1995.
[12] Bassett DC. Principles of polymer morphology. Cambridge: Cambridge University Press; 1981.
[13] Wunderlich B. Macromolecular physics, vol. 2. New York: Academic Press; 1976.
[14] Lu L, Alamo RG, Mandelkern L. Macromolecules 1994;27:6571.
[15] Zhou H, Wilkes GL. Polymer 1997;38:5735.
[16] Puig CC, Hill MJ, Odell JA. Polymer 1993;34:3402.
[17] Avrami M. J Chem Phys 1939;7:1103.
[18] Avrami M. J Chem Phys 1940;8:212.
[19] Avrami M. J Chem Phys 1941;9:177.
[20] Wasiak A. Chemtracts—Macromol Chem 1991;2:211.
[21] Ozawa T. Polymer 1971;12:150.
[22] Chiu F-C, Fu Q, Shih H-H. J Polym Sci Part B: Polym Phys 2002;40:325.
[23] Eder M, Wlochowicz A. Polymer 1983;24:1593.
[24] Harnisch K, Muschik H. Colloid Polym Sci 1983;261: 908.
[25] Minkova L, Mihailov M. Colloid Polym Sci 1989;267: 577.
[26] Gedde UW. Progr Colloid Polym Sci 1992;87:8.
[27] Ergoz E, Fatou JG, Mandelkern L. Macromolecules 1972;5:147.